CPCHFT 9 (16) 2277 – 2424 (2008) · ISSN 1439-4235 · Vol. 9 · No. 16 · November 10, 2008

D55711

A EUROPEAN JOURNAL

CHEMPHYSCHEM

OF CHEMICAL PHYSICS AND PHYSICAL CHEMISTRY

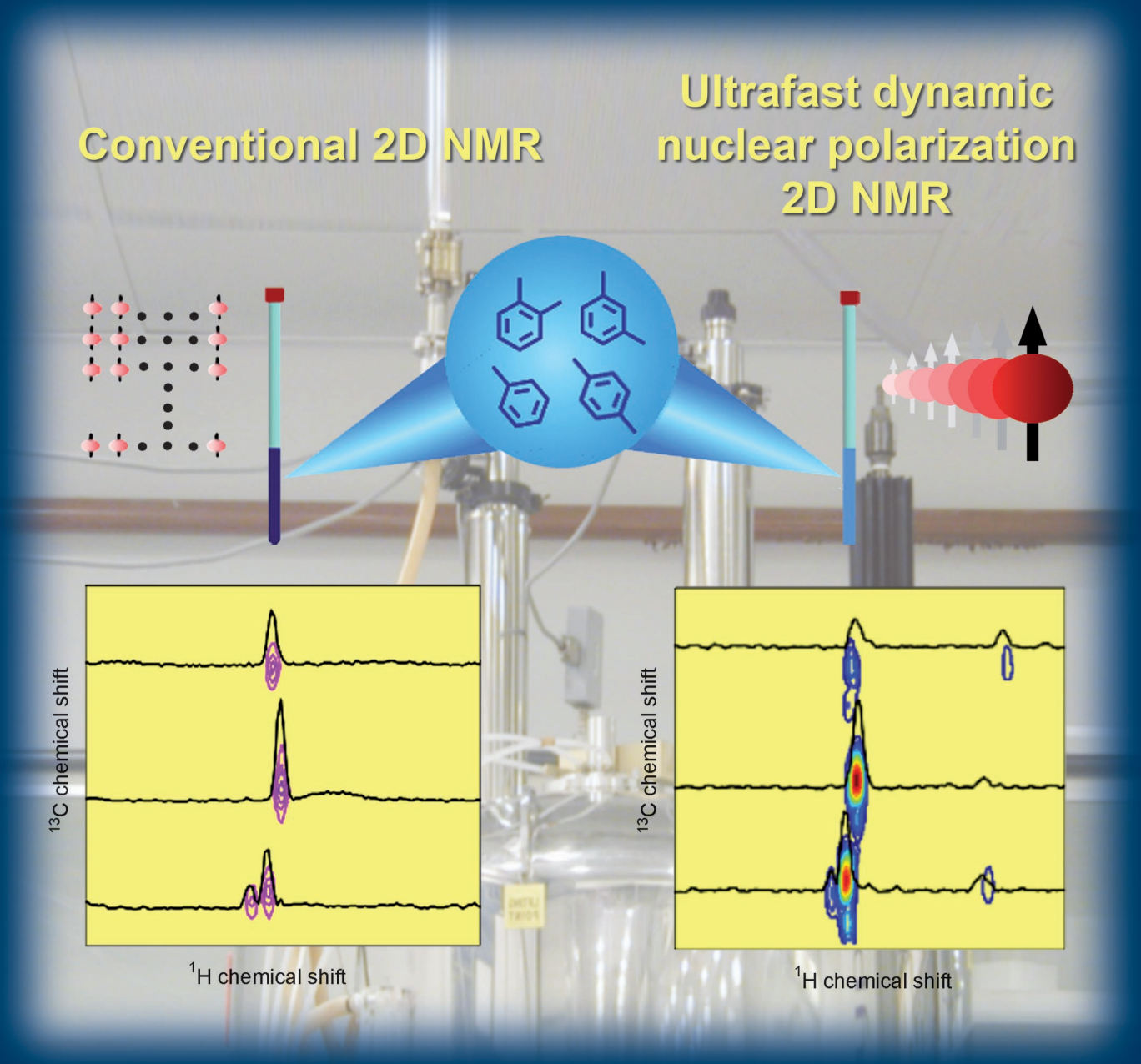

16/2008

Minireview: Monolayers on Metal Surfaces
(S. Baldelli)

Original Contributions: Hyperpolarized Ultrafast 2D NMR Spectroscopy
(L. Frydman and M. Mishkovsky)

Nuclear Spin Relaxation in Liquids from First Principles
(D. Sebastiani et al.)

ChemPubSoc Europe

www.chemphyschem.org

WILEY-VCH

CHEMPHYSCHEM

DOI: 10.1002/cphc.200800461

Progress in Hyperpolarized Ultrafast 2D NMR Spectroscopy

Mor Mishkovsky and Lucio Frydman*[a]

An important development in the field of NMR spectroscopy has been the advent of hyperpolarization approaches, capable of yielding nuclear spin states whose value exceeds by orders-of-magnitude what even the highest-field spectrometers can afford under Boltzmann equilibrium. Included among these methods is an ex situ dynamic nuclear polarization (DNP) approach, which yields liquid-phase samples possessing spin polarizations of up to 50%. Although capable of providing an NMR sensitivity equivalent to the averaging of about 1 000 000 scans, this methodology is constrained to extract its "superspectrum" within a single—or at most a few—transients. This makes it a poor starting point for conventional 2D NMR acquisition experiments, which require a large number of scans that are identical to one another except for the increment of a certain t_1 delay. It has been recently suggested that by merging this ex situ DNP approach with spatially encoded "ultrafast" methods, a suitable starting point could arise for the acquisition of 2D spectra on hyperpolarized liquids. Herein, we describe the experimental principles, potential features, and current limitations of such integration between the two methodologies. For a variety of small molecules, these new hyperpolarized ultrafast experiments can, for equivalent overall durations, provide heteronuclear correlation spectra at significantly lower concentrations than those currently achievable by conventional 2D NMR acquisitions. A variety of challenges still remain to be solved before bringing the full potential of this new integrated 2D NMR approach to fruition; these outstanding issues are discussed.

1. Introduction

The very low interaction energies that award nuclear magnetic resonance (NMR) its unique high resolution and noninvasiveness also deprive this spectroscopy of the sensitivity that characterizes competing physical techniques. One way to increase sensitivity involves operating at the highest possible magnetic field; yet even at the highest Zeeman couplings that can nowadays be reached by stable magnets, only about one in every 20 000 or so nuclei will contribute to the observable NMR signal.[1] Driven by this reality—compounded as it is by the diminishing returns delivered by existing superconducting magnet technologies—recent years have witnessed extensive efforts to devise alternatives to NMR spectroscopy that prepare nuclei in hyperpolarized states, that is, in states whose spin population differences depart from the usual $\approx 10^{-5}$ Boltzmann distributions and approach unity. These methods can deliver NMR spectra with unprecedented sensitivities, and include among others, chemical synthesis and parahydrogen,[2,3] optical pumping,[4,5] and microwave-driven transfers of magnetization from electrons to nearby nuclei by dynamic nuclear polarization (DNP).[6–9] DNP is arguably the most general among these methods: it only requires the irradiation of a small amount of co-dispersed free radical and, if performed under cryogenic conditions, it can deliver nuclear spin orders reaching up to nearly full polarization.[10–12] The most natural way to exploit such enhancement within the framework of an NMR experiment is to perform the DNP buildup in situ, that is, within the same phase and the same sample environment as will be later targeted by the NMR measurement. This logic has shown the highest promise and return within the framework of solid-state NMR spectroscopy,[10,13,14] but its application to enhance signals in a high-resolution liquid-state NMR setting is not that straightforward. Conspiring against this procedure is the relatively low electron→nuclear spin-order transfer efficiency characterizing liquids placed within a high-field setting, owing mainly to the unfavorable correlation times that then characterize molecules within the framework of the transfer needs.[7,9] This obstacle can be alleviated by carrying the nuclear polarization of the targeted liquid at low field strengths and then transferring the sample to higher fields for observation,[15–17] or by increasing the microwave powers to make up for the low transfer efficiency.[18]

An alternative way of achieving a DNP-enhanced liquid includes carrying out the pumping at low temperatures, on a frozen glassy medium where a number of polarizing mechanisms arise, and then rapidly transferring the sample into a solution phase while keeping the spins in their very highly ordered states. This rapid phase transfer can in turn be done either in situ assisted by a temperature jump (as for instance provided by a CO_2 laser[19]), or ex situ by sudden dissolution of the sample with a hot solvent vapor that then carries away the sample into an NMR scanner for conventional observation.[11,12,20] The availability of a commercial instrument capable of performing this latter DNP-based low-temperature hyperpo-

[a] M. Mishkovsky, Prof. L. Frydman
Department of Chemical Physics
Weizmann Institute of Science, 76100 Rehovot (Israel)
Fax: (+972) 8-9344123
E-mail: Lucio.Frydman@weizmann.ac.il

larization process and of rapidly melting the sample into the liquid state has begun to open valuable new opportunities in the fields of in vivo NMR spectroscopy and magnetic resonance imaging.[20–23]

In spite of being capable of delivering "supersignals" from hyperpolarized nuclear spin states in a variety of molecules, NMR experiments carried out within an ex situ DNP setting are limited by the fact that its targets can be analyzed only briefly: once the sample has changed state and been ejected from the hyperpolarizer into an NMR scanner, spins will return to their normal, weakly polarized Boltzmann equilibria within a relaxation time of about 3–4 T_1. In a 1D NMR framework this is not a constraining problem, as spectra can become available by performing a single $\pi/2$ excitation. Different, however, is the situation associated with 2D NMR acquisitions, which will normally demand the execution of a large number of complex pulse sequences including a relatively long data acquisition period, and differing solely in the duration of a t_1 interpulse delay somewhere within their midst.[24,25] In view of this constraint, we have recently begun exploring the potential that so-called "ultrafast" *n*D NMR experiments, capable of delivering full multidimensional NMR spectra within a single scan,[26–28] could offer upon being merged with DNP-based nuclear hyperpolarization methods. Preliminary results suggest that merging of ultrafast NMR and ex situ DNP experiments is indeed possible, and may lead to the acquisition of 2D NMR spectra on simple analytes within a fraction of a second and at submicromolar concentrations.[29] The purpose of the present article is to expand on those preliminary observations, and present a deeper description of the experimental principles, new potential, and challenges posed by the integration of ultrafast 2D NMR and DNP-enhancement methodologies. In particular, we focus on the possibility of exploiting the relatively long T_1 relaxation times exhibited by heteronuclei, which, starting with a substantial hyperpolarized signal, could then be transferred to bonded and nonbonded protons for a more sensitive and more informative detection. New heteronuclear single-quantum correlation (HSQC), heteronuclear multiple-quantum coherence (HMQC), and heteronuclear multiple-bond correlation (HMBC) pulse sequences based on this premise were developed, executed, and compared with conventional acquisitions to assess their signal-enhancing potential. It was thus found that, even when factoring in the relatively long pumping times required by the ex situ DNP procedure and the sensitivity losses associated with the sample transfer and single-scan 2D NMR data acquisition, an optimized operation of these new methods may enable one to access analyte concentrations that are lower by over an order of magnitude than those amenable from conventional counterpart experiments. This significant advantage, however, is only achieved in favorable cases; obstacles still remaining to be overcome for transforming this approach into a potential method of choice for the acquisition of 2D NMR spectra on small molecules are therefore noted.

Experimental Section

A variety of sequences combining the single-scan capabilities of ultrafast 2D NMR spectroscopy with the sensitivity enhancement of ex situ DNP were assayed by using an OIMBL Hypersense polarizer, akin to that described by Ardenkjær-Larsen et al.,[11] for performing the enhancement stage of the experiment, and a Varian Inova console equipped with an 11.7-T magnet for carrying out the NMR acquisitions. Given that the ex situ DNP procedure strongly biases the hyperpolarization towards the low-γ species, all the NMR measurements started once the sample had settled inside the spectrometer with the excitation of ^{13}C or ^{15}N heteronuclei (usually involving a $\pi/2$ pulse). A variety of schemes were then implemented to encode and transfer these heteronuclear coherences into protons for higher-sensitivity observation. All experiments were thus carried out using an inverse 5-mm NMR probe head, equipped with triple-axis *xyz* gradients.

Runs were started by mixing the sample to be studied with a small amount of an organic radical in a suitable glass-forming solvent. An aliquot of the resulting solution was then placed inside the helium-cooled variable-temperature insert located within the Hypersense polarizer's main 3.35-T magnet. This sample was cooled to 1.5 K and its free radical irradiated at about 94 GHz with $\approx$50–100 mW of microwave power. The length of the DNP pumping time varied between 1 and 12 h depending on the targeted compound, while the exact frequency of the microwave irradiation was periodically recalibrated by monitoring the response of a tuning sample every few weeks. After achieving a sufficient degree of hyperpolarization (not always optimized and/or exactly known), the irradiated samples were ejected from the Hypersense polarizer as a liquid, and carried by a stream of preheated vapors pushed by $\approx$3 atm of He gas into the NMR magnet. These chasing solvents were usually methanol and occasionally water, and they poured the sample into the observation probe in synchrony with a transistor–transistor logic command that started the operation of the NMR console. Whereas this transport of the DNP-pumped sample into the liquids probe began with about 4.0 mL of transferring solvent, the overall procedure resulted in only about 1.5 mL of sample in the final NMR tube—the remainder of solvent and sample remaining along the way. In view of these losses and of the ensuing variability in the dilution factors, ancillary spectrophotometric measurements relying on the strongly absorbing radical as internal standard were carried out to evaluate the final effective concentrations of the examined analytes.

2. Results

2.1. Ultrafast 2D NMR Spectroscopy: Principles and Preliminary Sudden-Injection Tests

Ultrafast 2D NMR spectroscopy replaces the serial time-based encoding occurring along the indirect domain of conventional 2D acquisitions, by an equivalent encoding of the spin evolution along a spatial axis. The essence of the method as applied to 2D acquisitions on liquid-state samples is summarized for completion in Figure 1. Lying at its core is the partitioning of the sample into a series of spatially independent subensembles, each of them encoding the kind of spin evolution that would normally be associated with a particular indirect-domain t_1 value. This partitioning can be achieved by applying a series of frequency-stepped or frequency-chirped radio-frequency (RF) pulses, which act in combination with suitably echoed

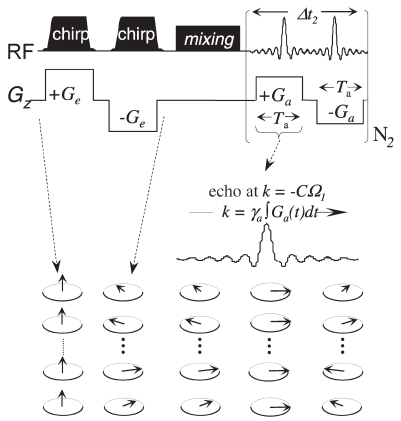

Figure 1. Principles involved in the retrieval of single-scan 2D NMR spectra. RF blocks indicate frequency-chirped pulses which, when coupled to suitable encoding magnetic field gradients G_e, achieve a sequential excitation/inversion of the spins along the gradient's direction and thereby shift-driven helical magnetization patterns along this axis (bottom). Following conventional mixing sequences, data are collected in the presence of oscillating acquisition gradients $\pm G_a$, capable of repetitively unwinding and winding the shift-induced spiral of spin packets encoded during the excitation. The sharp echoes that are then generated unveil an array of indirect-domain spectra, modulated in the direct domain by final evolution frequencies Ω_2 accessible through FT versus t_2.

magnetic-field gradients spreading out the spins' resonance frequencies along a particular direction, for instance, along the *z* axis. Such a combination allows one to imprint spatially heterogeneous shift-derived effects onto the spins' overall evolution; when considered within the framework of spin packets precessing in the Bloch sphere, these patterns represent a shift-induced Ω_1-dependent winding of the coherences along the spatial encoding coordinate (Figure 1, lower left). These windings will in general be characterized by a destructive interference among their constituents; during an acquisition stage, however, their spatially encoded information can be extracted by applying a suitable field gradient G_a that acts in combination with the data sampling. Such gradients will unwind the various helices that were subtended by the individual chemical sites, thus leading to observable echoes arising from constructive interference phenomena among spins positioned throughout the sample. The position of such echoes as a function of the $k = \gamma \int G_a(t)dt$ wavenumber will depend on the strengths of the Ω_1 interactions; their measurement allows one to map the indirect-domain spectra, thereby making out the k variable proportional to the indirect-domain frequency axis ν_1. Moreover, as such unwinding processes can be immediately reversed and repeated multiple times by alternating the sign of the G_a acquisition gradient, the direct-domain frequencies of the spins that are active during the final detection period can also be defined from the time modulation exhibited by such echoes. Subjecting the echo signals obtained during such a cyclic train of oscillating gradients to a suitable rearrangement and to a final 1D Fourier transform (FT) process along the direct domain[27] thereby leads to the desired 2D NMR spectrum—all of this within a single scan.

When attempting to couple this kind of NMR measurement with the ex situ DNP hyperpolarization procedure, one should notice the poor partnership that the various gradient-based spatial manipulations on which ultrafast 2D NMR spectroscopy relies will make with the turbulent motions that the sample undergoes as the polarizer rapidly injects it into the NMR observation tube. To evaluate potential interferences between the gradient-assisted spatial encoding/decoding procedures and the turbulence associated with this sudden sample injection, a series of stability tests were performed. To this end methanol and water were chosen as solvents, and a series of "mock" dissolutions were carried out focusing on how the parameters, such as the sample settling delays and the gradient oscillation characteristics, affect the realization of ultrafast 2D NMR experiments from Hypersense polarizer-ejected samples. Figure 2 summarizes some of these findings with a series of 2D $S(k/\nu_1,t_2)$ interferograms, in which echo lifetimes as a function of t_2 give a measure of the ideality of the experiment. These tests suggest that even upon employing the weakest possible encoding gradient strength G_e compatible with the experiment's realization, methanol injections require a wait of at least 0.7 s before applying the 2D sequence, while water-based injections require about twice this settling time. Figure 2D explores a different aspect of the experiment geared at defining the influence of using different acquisition oscillation periods T_a: the trend imposed by the injection-related turbulences suggests that interferograms collected using slower oscillation of the acquisition cycles become more prone to echo distortions than their shorter-T_a counterparts, a behavior that contrasts with what is observed when considering random Brownian motions.[30]

2.2. Hyperpolarized Ultrafast 2D NMR Experiments Based on Single-Bond Correlations

With the conditions for obtaining single-scan 2D NMR data following a sudden injection explored, we turned to investigate the potential opened up by DNP towards the recording of HSQC spectra. A previous study demonstrated that solvents such as pyridine could be observed in this manner;[29] once again we focus here on directly bonded ^{13}C–^{1}H HSQC, but geared this time at observing low-molecular-weight solutes that were pumped in a hyperpolarizing medium. The pulse sequence assayed in such experiments is shown in Figure 3A. It begins with a $\pi/2$ excitation of the low-γ heteronuclei, spatial encoding of the resulting coherences in a constant-time fashion by using a pair of frequency-swept π pulses,[31] passing of the ensuing information in nonquadrature mode to neighboring ^{1}H nuclei by the creation of $2H_zC_z$ spin-order terms, and the creation of an in-phase $\{^{13}C\}$-decoupled ^{1}H coherence for more sensitive and informative detection. This was done as is usual in single-scan 2D NMR spectroscopy in the presence of an oscillating decoding gradient, and was separated for its FT processed into two sets characterized by $\Delta t_2 = 2T_a$ that were subsequently recombined for improved signal-to-noise ratio (SNR). An application of this ultrafast 2D HSQC sequence to a

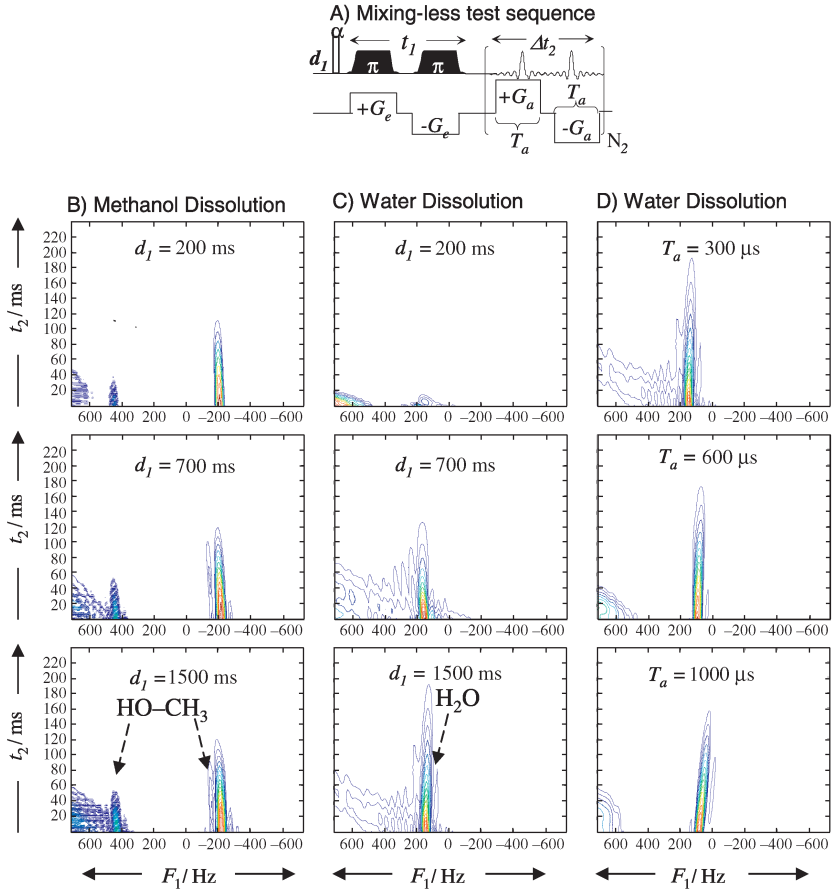

Figure 2. A) Mixing-less single-scan 2D NMR sequence used to assess the stability of ultrafast 2D NMR spectroscopy following a Hypersense®-driven sample dissolution. B,C) Unsheared 2D interferograms measured on "mock" dissolutions of methanol and water, respectively, for different settling times d_1. D) Same as (C) but with the interferogram monitored as a function of T_a. Unless stated otherwise, experimental parameters associated with the experiments included: $G_e = 2.5$ G cm^{-1}, $G_a = 15$ G cm^{-1}, $t_1^{max} = 15$ ms, $\alpha = 25°$, $SW_1 = 1480$ Hz, total acquisition time = 240 ms, $T_a = 300$ µs, $d_1 = 1.5$ s. The unmarked residual signal appearing in the lower-left corners of all panels are artifacts of nonencoded magnetization, which go away upon introducing a suitable purging pulse.

^{13}C–^{1}H correlation on hyperpolarized 3-methylsalicylic acid is illustrated in Figure 3B.

To gauge the potential sensitivity gains offered by this DNP-enhanced 2D HSQC experiment, we sought to make repeated comparisons against conventional 2D counterpart acquisitions. Given the relatively high costs involved when trying these systematic tests using the original, in vivo oriented radical/solvent combination suggested in ref. [11], an alternative system capable of yielding representative results for small-molecule studies was sought. Eventually we settled on the use of toluene and xylenes as polarizing media, and on αβ-bisdiphenylene-β-phenylallyl:benzene (BDPA) at 20 mM concentrations as the co-mixed radical.[32] Methylbenzenes are good organic solvents with the added advantage that their self-glassing behavior makes them suitable media for a cryogenic DNP buildup;[33] BDPA also presents multiple advantages including low cost, stability, good solubility, and a sharp EPR line resonating very close to the trityl species normally targeted by cryogenic DNP (94.087 vs 94.098 GHz in our specific setup). Substantial NMR signal enhancements, on the order of 10^4 for the ^{13}C resonances of the methylbenzenes, could be observed by pumping on BDPA in otherwise usual polarizer-based 1D NMR runs.

Figure 4 compares a DNP-enhanced ultrafast ^{13}C–^{1}H HSQC NMR spectrum collected using the sequence in Figure 3A for a 1:1:1:1 mixture of *o*-, *m*-, and *p*-xylenes plus toluene, against a conventional ^{1}H-excited/^{1}H-detected 2D HSQC spectrum collected on the same mixture dissolved in methanol using an optimized pulse sequence. In an effort to make measurements akin to one another, their total experimental times were chosen to be similar: a DNP pumping time of 1.5 h plus a negligible ≈0.3 s at the NMR spectrometer itself were employed for the hyperpolarized test, and a signal averaging time of ≈1.5 h within the spectrometer was used for the conventional acquisition. Also in an effort to make the influence of relaxation times and data points comparable, the spectral resolutions and widths along both domains were chosen to be similar for both 2D sets. As can be appreciated from the traces shown in Figure 4, the two data sets are not identical in terms of shifts, and minor cross-peak intensity heterogeneities arise due to certain DNP-induced biases. Their main disparity, however, rests in the very different solute concentrations that had to be used to obtain similar effective SNRs: ≈0.55 mM for each of the aromatics in the DNP-enhanced run against ≈20 mM for the conventionally acquired spectrum.

2.3. Hyperpolarized Ultrafast 2D NMR Experiments Using Multiple-Bond Correlations

When considering the potential gains that ex situ DNP could yield within an analytical setting, it is convenient to factor in the inherent heterogeneities that the sensitivity enhancement will show for the various chemical sites. Figure 5 illustrates these heterogeneities by comparing, for the compounds targeted in Figures 3 and 4, 1D ^{13}C NMR spectra measured following hyperpolarization vis-à-vis 1D traces collected for conventional thermal polarizations. Judging from the very different concentrations that had to be employed to collect these two data sets it is clear that all sites display, upon DNP, $>10^3$ enhancements in their signals; yet it is also clear that quaternary carbon atoms show systematically higher average signal en-

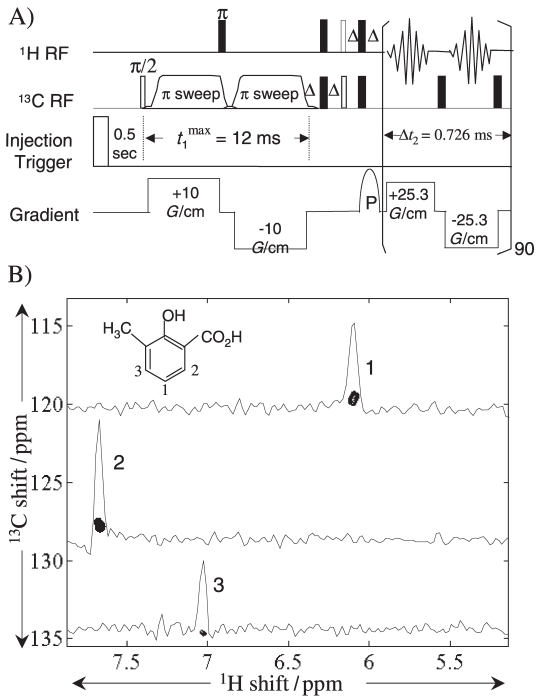

Figure 3. A) Pulse sequence and B) purely absorptive ultrafast 2D ^{13}C–^{1}H HSQC NMR spectrum arising from a 30 μL sample of hyperpolarized natural abundance 3-methylsalicylic acid. This analyte was co-frozen at a concentration of 450 mM with OX63 (15 mM) in a MeOH/[D_6]DMSO solution (1:1), irradiated for about 12 h at 94.107 GHz and 50 mW, and suddenly dissolved with [D_4]MeOD for NMR observation, thus leading to a final effective concentration of ≈6 mM. In (A), *P* denotes a small gradient purging pulse and $\Delta = 1.8$ ms. As in all the remaining ultrafast 2D experiments in this work, the data were digitized at a 2 μs per complex point dwell.

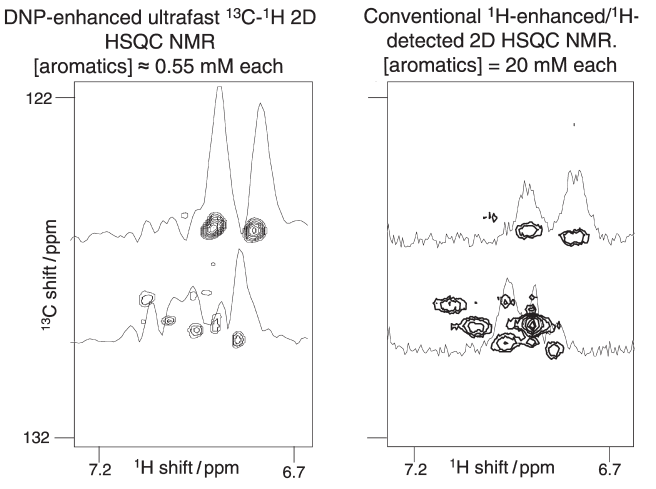

Figure 4. Comparison of two 2D ^{13}C–^{1}H HSQC NMR spectra (magnitude) measured on samples prepared by mixing *o*,*m*,*p*-xylene and toluene in a 1:1:1:1 ratio. The DNP-enhanced spectrum (left) was measured with a sample concentration of ≈0.55 mM for each component, whereas its conventional counterpart (whose pulse sequence was taken from the spectrometer's library) was measured at a sample concentration of ≈20 mM. The total experimental time in both tests was about the same, even though the amount of NMR spectrometer time for the left-hand acquisition was negligible. Spectra were zoomed so as to highlight the aromatic-region correlations, and two 1D cross sections were selected at the indicated ^{13}C positions for a better SNR assessment.

hancements than their protonated counterparts. This behavior can be rationalized by the fact that, even though the electron-induced enhancements happening in the cryogenic glass may be similar for all sites, the longer T_1 values that usually characterize nonprotonated ^{13}C atoms will help preserve the hyperpolarization of these sites upon porting the sample from the DNP to the NMR magnets. This in turn suggests the convenience of focusing on 2D NMR experiments whose correlations involve quaternary rather than protonated carbon atoms, for instance, on long-distance correlations to nonbonded protons of the kind arising in HMBC experiments.[25,34]

Figure 6 presents a sequence capable of implementing these 2D correlations between ^{13}C and ^{1}H through J^2_{CH} single-quantum coherences within a single scan. Features of this sequence include a direct ^{13}C excitation, suppression of one-bond ^{13}C–^{1}H correlations based on their transformation into multiple-quantum states following a delay $\frac{1}{2J^1_{CH}}$, a spatial encoding based on constant-time principles, a relatively long delay Δ tuned to enable the creation of two-bond $2H_zC_{x,y}$ antiphase terms, a pair of $(\pi/2)_{H,C}$ pulses that transform these terms into an amplitude-modulated antiphase ^{1}H coherence, and acquisition at the ^{1}H frequency while in the presence of an oscillatory decoding gradient. As in the HSQC case, ancillary purging gradients along orthogonal axes were included to filter out as much as possible potential ^{12}C–^{1}H signal contributions, but unlike those cases the t_1 and t_2 evolutions proceeded without heteronuclear decoupling. Figure 6 also compares, for the *o*,*m*,*p*-xylene/toluene (1:1:1:1) mixture, the HMBC traces arising from the sample in hyperpolarized and in thermally polarized 2D NMR experiments (the last one executed once again using an optimized sequence taken from the standard Varian software package).

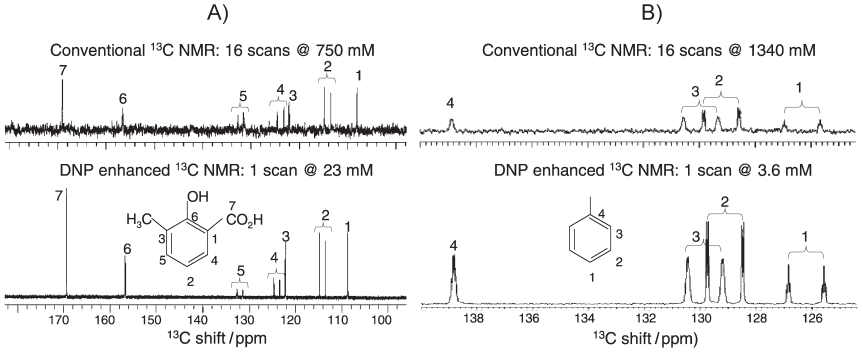

Figure 5. Comparison of conventional and hyperpolarized ^{1}H-coupled 1D ^{13}C NMR aromatic regions of 3-methylsalicylic acid (A) and toluene (B) dissolved in methanol. Notice the relative ratio between the analyte concentrations, as well as the higher signal shown by the quaternary carbon atoms due to their longer T_1 relaxation time.

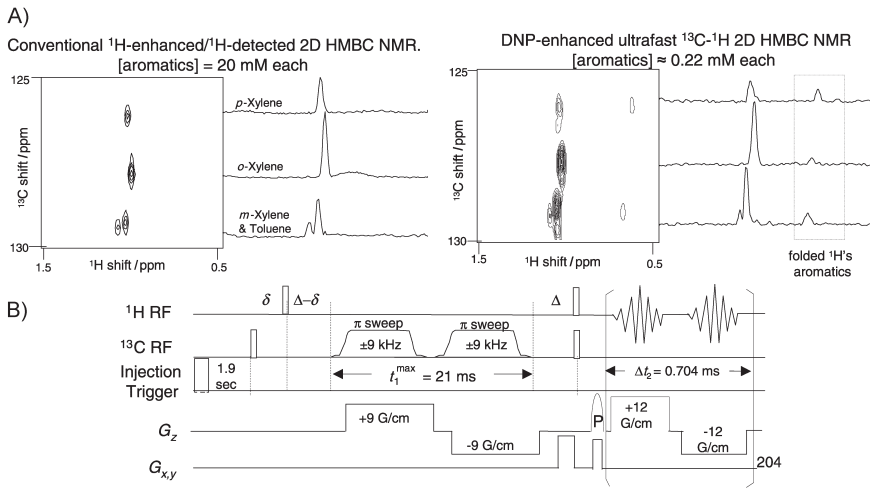

Figure 6. A) Comparison of DNP-enhanced ultrafast 2D ^{13}C–^{1}H and conventional 2D HMBC spectra measured on natural abundance *o*,*m*,*p*-xylene/toluene (1:1:1:1) mixtures. All 2D data are shown in magnitude mode and focus on the methyl-proton correlations. B) The sequence parameters of the ultrafast acquisition are as indicated; hollow lines denote $\pi/2$ pulses, the $G_{x,y}$ gradient pulses were added for coherence transfer selection purposes, and the Δ, δ delays were chosen as 3.2 and 15 ms, respectively, to optimize the multiple-bond transfer and the single-bond coherence suppression.

The parameters were set to involve comparable width and resolution characteristics in both the conventional and ultrafast acquisition, and the two 2D traces display comparable SNRs in the nonprotonated aromatic carbon correlations following comparable overall amounts of experimental time. The concentration in the conventional HMBC experiment, however, had to be increased by a factor of about 100 over that of the DNP-enhanced ultrafast acquisition to achieve such parity.

The reliance on long-distance couplings is of course not exclusive to ^{13}C: it is possible to exploit these for measuring 2D HMBC spectra starting from other hyperpolarized species. Figure 7 depicts an example of this with a single-scan ^{15}N–^{1}H HMBC experiment carried out on ^{15}N-choline chloride. As recently shown, the ^{15}N site of this compound undergoes efficient hyperpolarization by the trityl radical, with its ex situ transfer aided by long, $T_1 \geq 200$ s values.[35] The ensuing 2D NMR spectrum can therefore be obtained with good SNR by using ≈ 50 μM concentrations of the targeted analyte. In fact, it turns out that during a DNP-pumping process, nuclear species whose Larmor frequencies are different but within the usual line width of the electron spin radical (≈40 MHz for trityl), can become simultaneously hyperpolarized within the same pumping process. As shown by Day et al. it is then possible to exploit the hyperpolarization experienced by both species, one after the other, within the same pumping cycle.[36] Motivated by this observation, Figure 8 illustrates the performance of two consecutive ultrafast 2D NMR experiments based on the same hyperpolarized sample, but starting on the different heteronuclei present in a labeled urea molecule. Since the signal enhancement is usually lower for ^{15}N than for its ^{13}C counterpart, we began these measurements with a ^{15}N-triggered HSQC to ^{1}H, followed by a ^{13}CO–^{1}H ultrafast 2D correlation to complete two one-bond transfers. The results of this latter experiment are not optimal, yet still satisfactory when considering they required no additional polarization time.

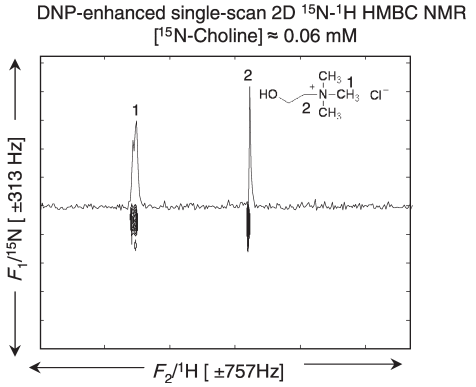

Figure 7. Single-scan ^{15}N–^{1}H 2D HMBC spectrum arising from hyperpolarizing ^{15}N-choline chloride (1 μL, 130 mM), co-frozen with OX63 (15 mM) within a $H_2O/[D_6]DMSO$ (1:1) solution, for about 3.75 h. Microwave irradiation was performed at 94.098 GHz and 100 mW, and rapid dissolution with $[D_4]$methanol led to an effective final concentration of 60 μM. An ultrafast HMBC sequence akin to that in Figure 6B was used, with settling time = 700 ms, $t_1^{max} = 15$ ms, $G_e = \pm 30$ G cm^{-1}, $T_a = 266$ μs, $G_a = \pm 8.4$ G cm^{-1}, filter bandwidth = 33 kHz, $N_2 = 333$.

2.4. Alternative Approaches to Hyperpolarized 2D NMR Spectroscopy

One possibility worth considering, upon weighing the opportunities that arise for collecting 2D NMR spectra on ex situ hyperpolarized samples, entails exploiting the relatively long-lived nature of longitudinal spin magnetizations and then monitoring, over a few times T_1, the full array of scans required for performing a 2D NMR experiment while utilizing small flip excitation angles.[37] These excitation pulses would once again have to begin on the heteronuclei, and optimal use of the spins' hyperpolarization suggests relying on sequences that employ the smallest possible number of pulses on this channel. With this goal in mind we decided to compare, on the same hyperpolarized target, the performance of a conventionally collected HMQC experiment correlating a ^{15}N atom with its directly bound ^{1}H (HMQC being a sequence which in its most basic form entails just a single ^{15}N pulse per t_1 increment;[38] Figure 9A) against an ultrafast 2D ^{15}N–^{1}H HSQC experiment of the kind detailed earlier. Moreover, to avoid potential T_1-driven distortions arising from relaxation during the 2D acquisition, the low-flip-angle RF pulses chosen for triggering each of the

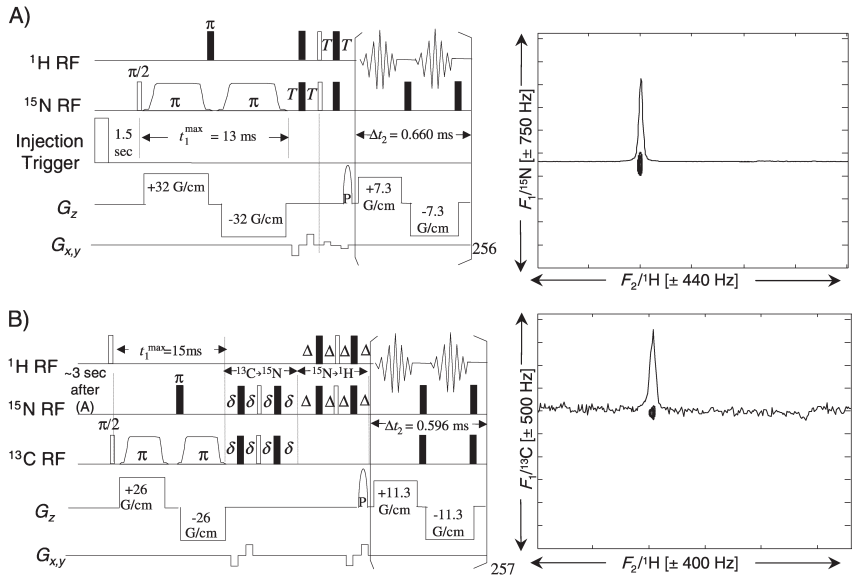

Figure 8. Two examples of ultrafast 2D NMR spectra measured through one-bond and two-bond ^{15}N–^{1}H and ^{13}C–^{1}H transfers on a single polarized ^{15}N,^{13}C-urea sample whose final concentration was 180 μM. The ^{15}N–^{1}H correlation was collected in a single scan; the ^{13}CO/^{1}H 2D correlation required two phase-cycled scans, which were carried out immediately after the first 2D scan. All nonselective $\pi/2$ and π pulses are as indicated; the T, δ, and Δ delays were set to 2.8, 2.8, and 8.3 ms, respectively, the $G_{x,y}$ gradient pulses were tuned to act as coherence pathway filters, and the initial ^{1}H $\pi/2$ in (B) was inserted to act as a homospoil background-suppression pulse.

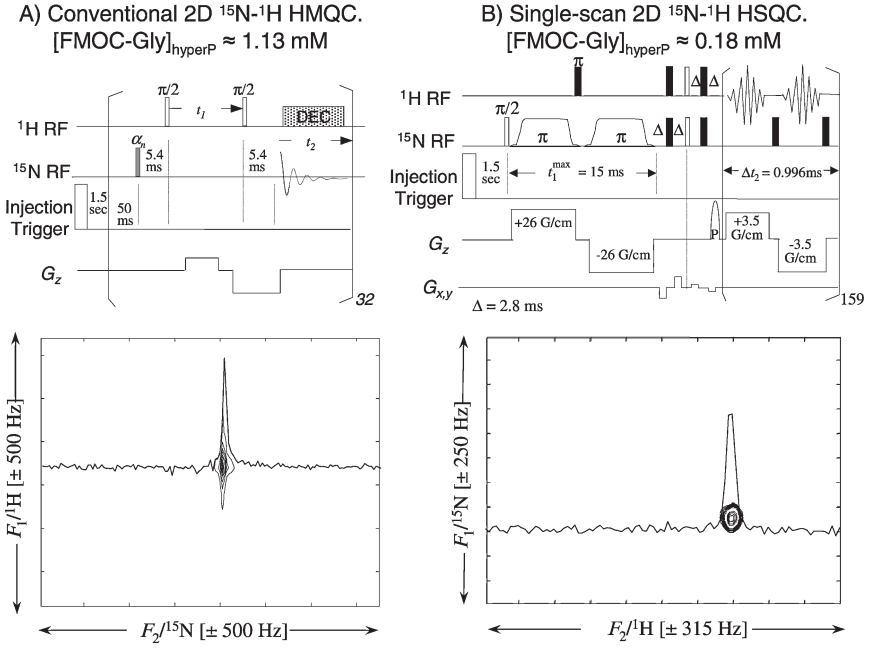

Figure 9. Comparison of a conventionally detected 2D HMQC spectrum acquired using low-flip-angle excitations on a hyperpolarized ^{15}N-labeled FMOC-Gly sample (A), and its single-scan 2D HSQC counterpart (B). (A) resulted from co-mixing 5 μL of a 0.5 M ^{15}N-labeled FMOC-Gly sample with 15 mM Finland radical in a [D_6]benzene/[D_6]DMSO (1:1) solution, and subjecting it to DNP at 94.098 GHz using 50 mW. (B) involved the same process, except that it started from 0.8 μL of the ^{15}N-labeled FMOC-Gly sample. Other experimental parameters involved were Δt_1 = 500 μs and t_2^{max} = 150 ms for the HMQC experiment, and Δ = 2.8 ms, filter bandwidth = 14 kHz, and t_2^{max} = 150 ms for HSQC.

32 t_1 temporal increments were adjusted individually in this comparison, so as to optimally tap the hyperpolarization over the full course of the 2D multiscan acquisition.[39] Figure 9 then compares, for a ^{15}N-labeled 9-fluorenylmethoxycarbonyl–glycine (FMOC-Gly) sample, representative ^{15}N–^{1}H 2D correlations afforded by the multiscan low-flip-angle HMQC vis-à-vis the single-scan HSQC. As can be appreciated, the two traces have comparable SNRs; the conventionally collected trace, however, needed nearly six times as high a sample concentration as the single-scan trace to achieve this parity. We are still exploring the reasons underlying these performance differences, which could be related to the decay of the hyperpolarization during the course of the ≈5 s long experiment and to the overall increase in noise levels that is associated with the multiscan averaging.

3. Discussion and Conclusions

We have surveyed some of the potential introduced by combining ex situ DNP-based hyperpolarization methods, capable of yielding outstanding SNRs but in a nonrepetitive mode, with ultrafast methods capable of exploiting these transient states for delivering 2D NMR data in a single scan. The results suggest that, when the ex situ DNP and the ultrafast experiments can both be executed with good performance, their combination endows at least certain kinds of 2D correlations with a sensitivity that exceeds the current state of the art by at least an order of magnitude. Moreover, this is achieved while demanding minimal amounts of actual spectrometer time. Unfortunately, the tests also revealed a number of shortcomings that will have to be overcome if a reasonable portfolio of applications is to develop out of this combination. Some of the problems observed stem from the current operation of the ex situ DNP procedure, which, having being optimized for polarizing certain metabolites, is still limited in the generality of the compounds it will

hyperpolarize and in its ability to deliver high polarizations for all sites with similar efficiencies (mostly, as mentioned, due to losses incurred upon transferring samples between the polarizing and the NMR magnets). Another limitation is the relatively large dilution that the sample undergoes upon shuttling between these two systems. A variety of efforts are currently focused on solving these important technical hurdles, which once dealt with will surely open valuable new opportunities in the use of hyperpolarized NMR spectroscopy for small-molecule, metabolite, and natural products research.

A separate set of problems arises from the ultrafast experiments themselves, particularly in terms of their implementation within the time course of events happening with the ex situ hyperpolarization. Most of these complications arise from having to operate on a suddenly injected sample, which forces us to deal with turbulences as well as with operation within an unlocked, undershimmed setting. As a result of these complications, all ^{13}C–^{1}H correlations illustrated in the previous section were obtained by measuring and combining in two (0°/180°) phase-cycled scans: not due to signal-averaging considerations, but rather because of the need for cycling at least these many scans for achieving a full elimination of an otherwise disturbing ^{1}H–^{12}C background and for achieving a more complete solvent suppression. This phase cycling is done at a cost to the SNR (see Figure 10), because once the hyperpolarized spin magnetization is pulsed upon within the first single-scan 2D NMR spectrum, a negligible amount of genuine signal remains in the second transient. We are currently looking for remedies to these various inefficiency problems including alternative spatial-encoding schemes, different pulsed-gradient purging combinations, sensitivity-enhancing schemes, and alternative forms of decoupling. In addition to these injection-related problems, a more fundamental set of complications arises from the inability of our current hardware to fit, with its available gradients, the full 200 ppm range of ^{13}C shifts that one would ideally like to cover in HSQC and HMBC experiments. This complication was bypassed in the present work by focusing on specific regions along the indirect domain; more general options (including fold-over procedures) will have to be developed for treating arbitrary compounds and mixtures.

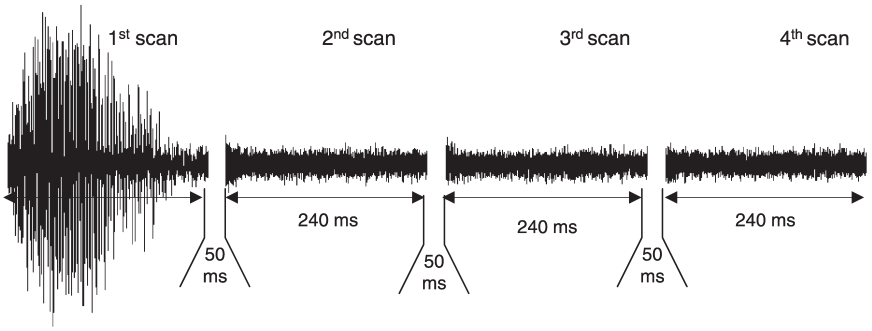

Figure 10. Series of free induction decays collected as described in the experiments for Figure 6 on a toluene sample (1 mM final concentration) after subjecting it to DNP and executing multiple ultrafast 2D HMBC acquisitions separated by short delays. Notice how the desired NMR echo signal arising from the hyperpolarized target molecule concentrates solely in the first scan; the small residual in subsequent scans dominates the SNR upon reducing the analyte concentration.

Acknowledgements

We are grateful to Andrew Sowerby, Joel Floyd, and Steve Reynolds (OIMBL, UK) for insight and assistance in the operation of the Hypersense polarizer. This work was supported by the US–Israel Binational Science Foundation (BSF 2004298), the Israel Academy of Sciences (ISF 1206/05), and the European Commission (EU-NMR contract No. 026145), and made possible by the generosity of the Perlman Family Foundation.

Keywords: correlation spectroscopy · dynamic nuclear polarization · hyperpolarization · NMR spectroscopy · ultrafast 2D NMR

[1] C. P. Slichter, *Principles of Magnetic Resonance,* Springer, New York, **1983**.
[2] C. R. Bowers, D. P. Weitekamp, *Phys. Rev. Lett.* **1986**, *57*, 2645.
[3] T. C. Eisenschmid, R. U. Kirss, P. P. Deutsch, S. I. Hommeltoft, R. Eisenberg, J. Bargon, R. G. Lawler, A. L. Balch, *J. Am. Chem. Soc.* **1987**, *109*, 8089.
[4] M. S. Albert, G. D. Cates, B. Driehuys, W. Happer, B. Saam, C. S. Springer, A. Wishnia, *Nature* **1994**, *370*, 199.
[5] G. Navon, Y.-Q. Song, T. Room, S. Appelt, R. E. Taylor, A. Pines, *Science* **1996**, *271*, 1848.
[6] T. R. Carver, C. P. Slichter, *Phys. Rev.* **1953**, *92*, 212.
[7] K. H. Hausser, D. Stehilk, *Adv. Magn. Reson.* **1968**, *3*, 79.
[8] A. Abragam, M. Goldman, *Nuclear Magnetism: Order and Disorder,* Oxford University Press, Oxford, **1982**.
[9] W. Muller-Warmuth, K. Meise-Gresch, *Adv. Magn. Reson.* **1983**, *11*, 1.
[10] L. R. Becerra, G. J. Gerfen, B. F. Bellew, J. A. Bryant, D. A. Hall, S. J. Inati, R. T. Weber, S. Un, T. F. Prisner, A. E. Mcdermott, K. W. Fishbein, K. E. Kreischer, R. J. Temkin, D. J. Singel, R. G. Griffin, *J. Magn. Reson. Ser. A* **1995**, *117*, 28.
[11] J. H. Ardenkjær-Larsen, B. Fridlund, A. Gram, G. Hansson, L. Hansson, M. H. Lerche, R. Servin, M. Thaning, K. Golman, *Proc. Natl. Acad. Sci. USA* **2003**, *100*, 10158.
[12] K. Golman, J. H. Ardenkjær-Larsen, J. S. Petersson, S. Månsson, I. Leunbach, *Proc. Natl. Acad. Sci. USA* **2003**, *100*, 10435.
[13] D. A. Hall, D. C. Maus, G. J. Gerfen, S. J. Inati, L. R. Becerra, F. W. Dahlquist, R. G. Griffin, *Science* **1997**, *276*, 930.
[14] K.-N. Hu, H.-H. Yu, T. M. Swager, R. G. Griffin, *J. Am. Chem. Soc.* **2004**, *126*, 10844.
[15] R. Gitti, C. Wild, C. Tsiao, K. Zimmer, T. E. Glass, H. C. Dorn, *J. Am. Chem. Soc.* **1988**, *110*, 2294.
[16] D. J. Lurie, J. M. S. Hutchison, L. H. Bell, I. Nicholson, D. M. Bussell, J. R. Mallard, *J. Magn. Reson.* **1989**, *84*, 431.
[17] E. R. McCarney, B. D. Armstrong, M. D. Lingwood, S. Han, *Proc. Natl. Acad. Sci. USA* **2007**, *104*, 1754.
[18] N. M. Loening, M. Rosay, V. Weis, R. G. Griffin, *J. Am. Chem. Soc.* **2002**, *124*, 8808.
[19] C. G. Joo, K. N. Hu, J. A. Bryant, R. G. Griffin, *J. Am. Chem. Soc.* **2006**, *128*, 9428.

[20] K. Golman, R. Zandt, M. Thaning, *Proc. Natl. Acad. Sci. USA* **2006**, *103*, 11270.
[21] A. P. Chen, M. J. Albers, C. H. Cunningham, S. J. Kohler, Y.-F. Yen, R. E. Hurd, J. Tropp, R. Bok, J. M. Pauly, S. J. Nelson, J. Kurhanewicz, D. B. Vigneron, *Magn. Reson. Med.* **2007**, *58*, 1099.
[22] S. E. Day, M. I. Kettunen, F. A. Gallagher, D.-E. Hu, M. Lerche, J. Wolber, K. Golman, J. H. Ardenkjaer-Larsen, K. M. Brindle, *Nat. Med.* **2008**, *457*, 940.
[23] F. A. Gallagher, M. I. Kettunen, S. E. Day, D.-E. Hu, J. H. Ardenkjær-Larsen, R. Zandt, P. R. Jensen, M. Karlsson, K. Golman, M. H. Lerche, K. M. Brindle, *Nature* **2008**, *457*, 940.
[24] J. Jeener, presented at *Ampere International Summer School II*, Basko Polje, Yugoslavia, September 1971. Lecture notes published in *NMR and More in Honor of Anatole Abragam* (Eds.: M. Goldman, M. Porneuf). (Les Editions de Physique, Les Ulis, France, **1994**).
[25] J. Keeler, *Understanding NMR Spectroscopy,* Wiley, Chichester, **2005**.
[26] L. Frydman, T. Scherf, A. Lupulescu, *Proc. Natl. Acad. Sci. USA* **2002**, *99*, 15858.
[27] L. Frydman, T. Scherf, A. Lupulescu, *J. Am. Chem. Soc.* **2003**, *125*, 9204.
[28] Y. Shrot, L. Frydman, *J. Am. Chem. Soc.* **2003**, *125*, 11385.
[29] L. Frydman, D. Blazina, *Nat. Phys.* **2007**, *3*, 415.
[30] Y. Shrot, L. Frydman, *J. Chem. Phys.* **2008**, *128*, 164513.
[31] P. Pelupessy, *J. Am. Chem. Soc.* **2003**, *125*, 12345.
[32] M. Afeworki, J. Schaefer, *Macromolecules* **1992**, *25*, 4092.
[33] C. Alba, L. E. Busse, D. J. List, C. A. Angell, *J. Chem. Phys.* **1990**, *92*, 617.
[34] A. Bax, M. F. Summers, *J. Am. Chem. Soc.* **1986**, *108*, 2093.
[35] C. Gabellieri, S. Reynolds, A. Lavie, G. S. Payne, M. O. Leach, T. R. Eykyn, *J. Am. Chem. Soc.* **2008**, *130*, 4598.
[36] I. J. Day, J. C. Mitchell, M. J. Snowden, A. L. Davis, *Magn. Reson. Chem.* **2007**, *45*, 1018.
[37] C. Ludwig, M. Saunders, U. Günther, *49th Experimental NMR Conference*, Poster #183, Asilomar, California, March **2008**.
[38] L. Müller, *J. Am. Chem. Soc.* **1979**, *101*, 4481.
[39] K. Nagashima, *J. Magn. Reson.* **2008**, *190*, 183.

Received: July 23, 2008
Published online on October 10, 2008

